



Year: 2019

MicroRNA-125b Regulates Fibroblast Apoptosis Proliferation in Systemic Sclerosis

Kozlova, Anastasiia ; Pachera, Elena ; Maurer, Britta ; Jüngel, Astrid ; Distler, Jörg H W ; Kania, Gabriela ;
Distler, Oliver

Abstract: **OBJECTIVE** The aim of the study was to analyze the expression, regulation and role of microRNA-125b (miR-125b) in systemic sclerosis (SSc). **METHODS** MiR-125b expression was assessed by qPCR on RNA from dermal fibroblasts and whole skin biopsies of healthy controls (HC) and SSc patients. To identify downstream effectors, RNA from HC fibroblasts after miR-125b knockdown was sequenced and further validated using qPCR and Western blot. Fibrosis, apoptosis and proliferation were assessed by Caspase-Glo 3/7 assay, Western blot, immunofluorescence for cleaved caspase 3 and Annexin V live assay in dermal fibroblasts. **RESULTS** Expression of miR-125b was significantly downregulated in SSc skin biopsies by 53% (median 0.47, Q 0.35, 0.69; $p < 0.001$) and in SSc dermal fibroblasts by 47% (median 0.53, Q 0.36, 0.58; $p < 0.001$) in comparison to HC skin biopsies and fibroblasts, respectively ($n=10$, each). Treatment with the histone deacetylase inhibitors trichostatin A and tubastatin significantly decreased the expression of miR-125b in dermal fibroblasts. MiR-125b knockdown significantly reduced cell proliferation and α SMA expression at RNA and protein levels. RNAseq identified BAK1, BMF and BBC3 as potential targets of miR-125b. qPCR confirmed that knockdown of miR-125b upregulated these genes ($n=12$, $p < 0.01$). BAK1 showed the strongest induction confirmed on protein level ($n=10$, $p < 0.01$). Consequently, miR-125b knockdown increased apoptosis compared to scrambled controls. Accordingly, miR-125b overexpression decreased apoptosis. **CONCLUSION** MiR-125b is downregulated in SSc skin and primary SSc dermal fibroblasts. MiR-125b downregulation increases apoptosis, decreases proliferation and α SMA expression in dermal fibroblasts indicating a compensatory, anti-fibrotic mechanism as a potential novel therapeutic option. This article is protected by copyright. All rights reserved.

DOI: <https://doi.org/10.1002/art.41041>

Posted at the Zurich Open Repository and Archive, University of Zurich

ZORA URL: <https://doi.org/10.5167/uzh-172736>

Journal Article

Accepted Version

Originally published at:

Kozlova, Anastasiia; Pachera, Elena; Maurer, Britta; Jüngel, Astrid; Distler, Jörg H W; Kania, Gabriela; Distler, Oliver (2019). MicroRNA-125b Regulates Fibroblast Apoptosis Proliferation in Systemic Sclerosis. *Arthritis and Rheumatology*, 71(12):2068-2080.

DOI: <https://doi.org/10.1002/art.41041>

DR. JÖRG H.W. DISTLER (Orcid ID : 0000-0001-7408-9333)

DR. OLIVER DISTLER (Orcid ID : 0000-0002-2413-1959)

Article type : Full Length

MicroRNA-125b Regulates Fibroblast Apoptosis and Proliferation in Systemic Sclerosis

Anastasiia Kozlova PhD¹, Elena Pachera PhD¹, Britta Maurer MD¹, Astrid Jüngel PhD¹, Jörg H.W. Distler MD², Gabriela Kania PhD^{1x}, Oliver Distler MD^{1x}

Author affiliations

¹Center of Experimental Rheumatology, Department of Rheumatology, University Hospital Zurich, Switzerland

²Department of Internal Medicine 3, Rheumatology and Immunology, Friedrich-Alexander University Erlangen-Nuremberg, Germany

x= contributed equally

Correspondence to

Prof. Dr. Oliver Distler, Department of Rheumatology, University Hospital Zurich, Gloriastrasse 25, 8091 Zurich, Switzerland; Oliver.Distler@usz.ch; Tel: +41 44 255 29 70.

This article has been accepted for publication and undergone full peer review but has not been through the copyediting, typesetting, pagination and proofreading process, which may lead to differences between this version and the Version of Record. Please cite this article as doi: 10.1002/art.41041

This article is protected by copyright. All rights reserved.

Keywords Systemic sclerosis, microRNA, apoptosis, fibroblasts, miR-125b

Funding Institutional support, Theodor und Ida Herzog-Egli-Foundation, Helmut Horten Foundation, Orphan Disease Program grant from European League Against Rheumatism (EULAR), SNF grant 310030_166259.

ABSTRACT

Objective: The aim of the study was to analyze the expression, regulation and role of microRNA-125b (miR-125b) in systemic sclerosis (SSc).

Methods: MiR-125b expression was assessed by qPCR on RNA from dermal fibroblasts and whole skin biopsies of healthy controls (HC) and SSc patients. To identify downstream effectors, RNA from HC fibroblasts after miR-125b knockdown was sequenced and further validated using qPCR and Western blot. Fibrosis, apoptosis and proliferation were assessed by Caspase-Glo 3/7 assay, Western blot, immunofluorescence for cleaved caspase 3 and Annexin V live assay in dermal fibroblasts.

Results: Expression of miR-125b was significantly downregulated in SSc skin biopsies by 53% (median 0.47, $Q_{1,3}$ 0.35, 0.69; $p < 0.001$) and in SSc dermal fibroblasts by 47% (median 0.53, $Q_{1,3}$ 0.36, 0.58; $p < 0.001$) in comparison to HC skin biopsies and fibroblasts, respectively (n=10, each). Treatment with the histone deacetylase inhibitors trichostatin A and tubastatin significantly decreased the expression of miR-125b in dermal fibroblasts. MiR-125b knockdown significantly reduced cell proliferation and α SMA expression at RNA and protein levels. RNAseq identified *BAK1*, *BMF* and *BBC3* as potential targets of miR-125b. qPCR confirmed that knockdown of miR-125b upregulated these genes (n=12, $p < 0.01$). BAK1 showed the strongest induction confirmed on protein level (n=10, $p < 0.01$). Consequently, miR-125b knockdown increased apoptosis compared to scrambled controls. Accordingly, miR-125b overexpression decreased apoptosis.

Conclusion: MiR-125b is downregulated in SSc skin and primary SSc dermal fibroblasts. MiR-125b downregulation increases apoptosis, decreases proliferation and α SMA expression in dermal fibroblasts indicating a compensatory, anti-fibrotic mechanism as a potential novel therapeutic option.

Systemic sclerosis (SSc) is a multiorgan, chronic autoimmune disease characterized by fibrosis of the skin and internal organs. Skin fibrosis is a strong surrogate of overall disease progression and survival with major impact on the physical function and quality of life of the patients. Although novel targeted therapies are in advanced clinical development, there is no FDA or EMA approved anti-fibrotic therapy available to date(1, 2).

In SSc, tissue injury leading to microvascular damage and release of inflammatory factors stimulates transforming growth factor beta 1 (TGF β 1) production and differentiation of dermal resident fibroblasts into activated myofibroblasts. Myofibroblasts produce excessive amounts of extracellular matrix (ECM) such as collagens and fibronectin. Under physiological conditions, this process is terminated by reparative mechanisms driving the myofibroblasts into apoptosis. In the pathological course of SSc, persistent TGF β 1 signaling protects myofibroblasts from apoptosis and facilitates fibrosis(3-5).

Apoptosis plays a prominent role in many biological processes including autoimmunity. The BCL-2 family of proteins is at the center of the mitochondrial apoptotic pathway and consists of pro- and anti-apoptotic members. Their ratio determines whether a cell survives or dies(6, 7). The BCL-2 family is divided into three groups by function and structural homology: apoptosis-sensitizers (BH3-only proteins such as BMF and PUMA), anti-apoptotic proteins (e.g. BCL-2) and apoptosis-executors (BAX and BAK)(8). BH3-only proteins exert their pro-apoptotic effects via two alternative ways: by neutralizing anti-apoptotic proteins or by activating directly the apoptosis effectors BAK and BAX(9).

MiRs are small non-coding RNAs, which regulate specific target gene expression by repressing mRNA translation or by direct degrading of mRNA(10-12). One miR is able to repress up to hundreds of genes and one gene can be repressed by several miRs. Such a fine-tuned powerful machinery is evolutionally developed and is one of the pillars of post-transcriptional regulation(13).

Screening assays with small number of patients suggested that miR-125b might be differentially expressed in the skin of patients with SSc compared to healthy controls(14-16). In cardiac fibrosis, miR-125b directly affects fibroblast-to-myofibroblasts transition(17). In cancer, it may play a dual, tissue-specific role in increasing or decreasing cell apoptosis and proliferation(18-20). Therefore, we hypothesized that miR-125b might play an important role in the pathophysiology of SSc, and aimed to characterize its differential expression and function in SSc.

MATERIALS AND METHODS

Patients and biopsy specimens

All research on human derived samples was in compliance with the Helsinki Declaration. The approval of the local ethics committee was obtained for the Department of Rheumatology, University Hospital Zurich, Switzerland (approved ethical application KEK-ZH-Nr. 2014-0197).

Three millimeter punch biopsies were taken from the forearm skin of SSc patients (Supplementary Table 1) or healthy controls (Supplementary Table 2) after signed informed consent from patients and healthy donors. All patients fulfilled the EULAR/ACR 2013 classification criteria(21). The subset of the disease was defined according to LeRoy(22). Additionally, skin was taken from healthy, uninvolved skin of various surgery sites of donors having a condition not related to SSc (e.g. patients for plastic surgery operations) and considered to be healthy control skin. Biopsies were divided by half. One half was used for fibroblast isolation, the other half for RNA extraction.

Cell culture and stimulation experiments

Primary human dermal fibroblasts were obtained by outgrowth culture and used at passages 4-10 in standard culture conditions as described before(23). Briefly, half of the punch biopsy was cut in smaller pieces and distributed on the surface of the culture plate to dry and attach to the surface. Low glucose Dulbecco's Modified Eagle Medium (DMEM, Sigma-Aldrich) containing 50 U/mL Penicillin and 50 µg/mL Streptomycin (Gibco), 10% fetal bovine serum (10% FBS, Gibco) and 100 µM 2-mercaptoethanol (Gibco) (10% DMEM) was added and used for culture. Starvation medium containing 1% FBS was used in some experiments. Cells were maintained in 5% CO₂ humid 37°C incubator with medium change every 3-4 days. Cells were split after they reached 90-100% confluence.

For stimulation experiments various cytokines and epigenetic stimuli were used, such as: TGFβ₁ (0.1-10 ng/ml, Peprotech), activin (10 ng/ml, R&D Systems), PDGF (20 ng/ml, Peprotech), IL-1β, -4, -13 and IL-17A (all 10 ng/ml, ImmunoTools), TNFα (10 ng/ml, R&D Systems), TSA (0.33-4 µM, Sigma-Aldrich), VPA (1-4 µM, Sigma-Aldrich) and TBA (5-25 µM, Sigma-Aldrich).

RNA isolation and quantitative real-time PCR (qPCR)

Half of the 3mm punch biopsy was placed into RNAlater™ solution (ThermoFisher Scientific), stored overnight at +4°C to ensure proper penetration of the tissue, then moved to -80°C until the extraction. Half of 3mm punch biopsy was homogenized with Minilys by Bertin Technologies with 30sec homogenizing/30sec break 3 cycle on ice until the tissue was completely homogenized. Homogenates were proceeded to RNA extraction with the Qiagen RNeasy Fibrous Tissue kit according to the manufacturer's protocol including in-column DNA digestion.

Expression of miR-125b was assessed separately in epidermis and dermis of paraffin-embedded skin. For this, we manually separated epidermis from dermis and extracted RNA separately with RecoverAll™ Total Nucleic Acid Isolation kit (Ambion) following the manufacturer's protocol.

For basal microRNA expression analysis, dermal fibroblasts from passage 4 were collected and extracted with the Zymo Quick-RNA™ MicroPrep RNA isolation kit, including in-column DNA digestion. Reverse transcription and qPCR were performed according to Chen et al.(24) and described in detail in supplementary file.

Transfection and RNA sequencing

For transfections, we used the following assays: mirVana™ hsa-miR-125b-5p inhibitor (Assay ID MH10148 / #4464085) – anti-125b, mirVana™ miRNA Inhibitor Negative Control #1 (#4464077) – anti-scr, mirVana™ miRNA mimic hsa-miR-125b-5p (Assay ID MC10148 / #4464067) – pre-125b and mirVana™ miRNA mimic Negative Control #1 (#4464058) – pre-scr, all from ThermoFisher Scientific; for BAK1 knockdown FlexiTube GeneSolution (1027416/Cat no GS578 from Qiagen) and respective siRNA negative control were used at the concentration 0.4 nM. Cells were transfected according to the RNAiMAX transfection procedure with Lipofectamine® RNAiMAX reagent (ThermoFisher Scientific) and 100nM RNA final concentration. Functional assays and harvesting cells for RNA or proteins were performed 24, 48 and 72 hours after transfection. RNA sequencing methodology is described in supplementary file.

Western blot, Pro-Collagen Ia1 ELISA and SircolTM Collagen assay

Western blots (WB) were performed using the following primary antibodies: anti-BAK1 (1:500, ab32327 Abcam), anti-cleaved caspase 3 (1:200, ab2302 Abcam), anti-alpha smooth muscle actin (α SMA) (1:1000, A2547 Sigma) and GAPDH as loading control (1:10⁵000, #2118 Cell signaling) according to standard protocols(25). Proteins for cleaved caspase 3 WB were harvested 48 hours after transfection and 16 hours of treatment with 2 μ M of staurosporine (STP – apoptosis inducer) (S5921, Sigma). The ImageJ program was used to semi-quantify the signal.

The human Pro-Collagen Ia1 (Col1a1) ELISA (R&D systems) and SircolTM (Biocolor Life Science Assays) were used to assess collagens' content in cell supernatants according to manufacturers' protocols. All conditions were done in triplicates. Mean absorbance and collagen concentration were calculated using the standard curve. Anti-scr unstimulated cells served as controls. All experimental conditions were calculated as fold change to controls.

Immunofluorescence (α SMA, cleaved caspase 3)

For immunofluorescence staining, 2'000 cells were seeded in 8-well glass chamber slides (Lab-Tec). On the next day they were transfected with anti-125b or anti-scr controls. Furthermore, cells were stimulated with 10ng/ml TGF β (for α SMA staining) or with 200 μ M (S)-(+)-camptothecin (C9911, Sigma) to stimulate apoptosis (for cleaved caspase 3 staining) 24 hours after transfection. After respective fixation and blocking, cells were incubated with primary anti- α SMA antibody (1:100, A2547 Sigma) for 1 hour at room temperature or anti-cleaved caspase 3 antibody (1:300, #9661, Cell Signaling) overnight at 4°C. The following secondary antibodies were used: goat anti-mouse IgG (H+L), labeled with Alexa Fluor 546 (1:400, ThermoFisher Scientific) for α SMA staining or goat anti-rabbit IgG (H+L), labeled with Alexa Fluor 546 (1:400, ThermoFisher Scientific) for cleaved caspase 3 staining. To visualize cell nuclei, slides were counterstained with DAPI. Pictures were taken with the Olympus BX53 microscope equipped with a DP80 camera. Confocal pictures for cleaved caspase 3 immunofluorescence staining were taken with the Leica SP8 inverse microscope.

Caspase Glo® 3/7 and Real Time-Glo™ Annexin V assays

To assess apoptosis, the Caspase Glo® 3/7 assay (Promega) was used to measure the activity of the key effector caspases 3 and 7. Cells were seeded at a density of 2'000 cells/well in 96-well white-wall plates. On the next day, cells were transfected with anti-125b or anti-scr control, and pre-125b or pre-scr control, respectively. Cleaved caspases 3/7 activity was assessed 24, 48 and 72 hours after transfection. Two hundred μ M (S)-(+)-camptothecin (C9911, Sigma) was added 18 hours before the assay to stimulate apoptosis. Caspase-Glo® reagent was distributed to the wells, carefully mixed and left to incubate in the dark for 90 minutes at room temperature. Luminescent signals were measured with the Synergy HT microplate reader (BioTek).

The Real Time-Glo™ Annexin V Apoptosis kit (Promega) was used to assess the progression of apoptosis after transfection in real time. Cells were seeded at a density of 2'000 cells/well in 96-well white-wall plates and were allowed to settle overnight. Twenty-four hours after transfection, cells were stimulated with 2 μ M staurosporine (S5921, Sigma, apoptosis inducer) and the annexin V signal was recorded every 70 min, between 5 and 16 hours after apoptosis stimulation.

All conditions were done in quadruplicates. The mean luminescence was calculated, and anti-scr transfected unstimulated cells served as controls. All experimental conditions were calculated as fold change to controls.

Real time proliferation assay

Real-time cell analysis (RTCA) was used to assess the proliferation after anti-125b transfection in real time. Cells were seeded in the E-plates® (ACEA Biosciences, San Diego, CA), transfected with anti-125b or anti-scrambled control, and stimulated with TGF β . The cell index was measured every half an hour up to one week. The ACEA RT-CES 16 \times E-Plate Station (ACEA Biosciences) was used in the incubator at 37°C and 5% CO₂. The RTCA software was used to analyze the data.

Statistical analysis

Data are presented as median \pm interquartile range. Non-parametric tests (e.g. Mann-Whitney, Wilcoxon tests, etc.) were used for assessing statistical significance ($p < 0.05$). The statistical analysis was performed using GraphPad Prism 7.

RESULTS

MiR-125b expression and regulation in SSc skin and primary dermal fibroblasts

In all analyzed samples, which were obtained from the patients with different disease subtypes (diffuse and limited) and different disease duration (1 to 10 years) (Supplementary Table 1. Characteristics of SSc patients), miR-125b was consistently downregulated in SSc skin biopsies (n=10, median 0.47, $Q_{1,3}$ 0.35, 0.69; $p < 0.001$) compared with HC skin (n=10) (Fig. 1A). The related family member miR-125a was not differentially expressed (data not shown). Similarly, miR-125b expression was reduced in cultured dermal SSc fibroblasts (median 0.53, $Q_{1,3}$ 0.36, 0.58; n=10, $p < 0.001$) compared with HC fibroblasts (n=10) (Fig. 1B). In addition, the expression of miR-125b was downregulated in both SSc dermis and epidermis from paraffin fixed skin compared to healthy donors (Suppl. Fig. 1). Thus, these data indicate that miR-125b is consistently downregulated in SSc skin across different disease stages, compartments and cell types including fibroblasts.

We further showed that key cytokines active in SSc (TGF β 1, TGF β 1+Activin, PDGF, IL-1 β , IL-4, IL-13, IL-17A, TNF α) did not modulate the expression of miR-125b in primary dermal fibroblasts (Suppl. Fig. 2 and data not shown). In contrast, trichostatin A (TSA), a pan-inhibitor of histone deacetylases (HDAC), downregulated miR-125b expression in a time- and dose-dependent manner in SSc and HC fibroblasts (Fig. 1C-F). There was no significant effect on the expression of miR-125b after stimulation with valproic acid, an inhibitor of class I HDAC (Suppl. Fig. 3). However, tubastatin A (TBA), an inhibitor of class II HDAC, downregulated miR-125b in a dose-dependent manner (Fig. 1G-H). TBA specifically downregulated miR-125b, but not unrelated miRs, as shown for miR-342 (Fig. 1I-J).

Taken together, the downregulation of mir-125b appeared to be independent from main cytokines playing an emergent role in SSc. However, the experiments indicated an epigenetic regulation of this miR.

Role of miR-125b in fibrosis

To characterize the functional role of miR-125b in the pathophysiology of SSc, we performed targeted inhibition and overexpression using *mirVana*TM antagomirs and pre-miRs. Transfection with anti-125b resulted in more than 99% downregulation of miR-125b expression (Suppl. Fig. 4A-B), while transfection with pre-125b caused an average 7.6-fold increase in the expression of miR-125b in HC and SSc fibroblasts 24-72 hours post transfection (Suppl. Fig. 4C-D).

The expression levels of α SMA and collagens I, III, V were analyzed to assess the effect of miR-125b downregulation on key fibrotic parameters. There was no change of the expression of collagens on the mRNA and protein level after miR-125b downregulation with or without TGF β 1 stimulation in HC and SSc fibroblasts (Suppl. Fig. 5A-H). TGF β 1 stimulation caused a median 44% lower expression (0.56-fold, $Q_{1,3}$ 0.51, 0.6, $p < 0.01$) of ACTA2 (α SMA gene) in anti-125b transfected cells compared to anti-scr controls with and without starvation (Fig. 2A-B), while no difference was observed on the basal levels without TGF β 1 stimulation. Accordingly, HC fibroblasts transfected with anti-125b and stimulated with TGF β 1 showed a significantly reduced expression of α SMA protein content and fiber formation without starvation (Fig. 2C, E) and even stronger reduction with starvation (Fig. 2D), which was further confirmed in SSc fibroblasts (5.32-fold, $Q_{1,3}$ 3.17, 6.34 in comparison with anti-scr 9.05-fold, $Q_{1,3}$ 7.94, 9.9, $p < 0.01$) (Fig. 2F). In addition, miR-125b overexpression caused an upregulation of α SMA protein already on the basal level (3.77-fold, $Q_{1,3}$ 2.2, 3.82, $p < 0.01$), which increased further after stimulation with TGF β 1 (Fig. 2G).

Thus, miR-125b affected α SMA expression on the mRNA and protein level, but did not induce collagens.

RNA deep sequencing unraveled potential pro-apoptotic targets of miR-125b

To identify direct targets of miR-125b in the pathogenesis of SSc, we downregulated miR-125b with antagomirs in HC fibroblasts, mimicking the downregulation observed in SSc skin. RNA was isolated 24 hours later and subjected to deep RNA sequencing. For assessing differentially expressed genes the following criteria were used: FPKM > 5 , fold change > 1.2 , p -value < 0.01 (Suppl. Fig. 6A). In total, 163 genes were differentially expressed (36 downregulated and 127 upregulated). Further, we performed computational prediction algorithms for miR targets (TargetScan and MiRWalk) on the newly identified

Accepted Article

differentially expressed genes. Out of 163 differentially expressed genes, 59 were identified as predicted targets of miR-125b, which indicated successful enrichment for miR-125b targets in this experimental setting. Hierarchical clustering of predicted targets (Suppl. Fig. 6B) allowed us to choose consistently upregulated targets for further validation. Consequently, *BAK1*, *BMF* and *BBC3*, all members of the mitochondrial apoptotic pathway, were identified (Suppl. Table. 5). qPCR showed that at 24, 48 and 72 hours after downregulation of miR-125b, all three target genes were consistently upregulated in HC fibroblasts (1.21-1.79-fold up, $p < 0.001$) (Fig. 3A). Similarly, these pro-apoptotic genes were upregulated 48 and 72 hours after transfection in SSc fibroblasts. At 24 hours, *BAK1* and *BMF* were upregulated (1.53 and 1.47-fold change, respectively, $p < 0.05$), but not *BBC3* (1.15-fold, $p = 0.21$) (Fig. 3B).

To further support a regulation of *BAK1*, *BMF* and *BBC3* by miR-125, we next overexpressed miR-125b in SSc and HC fibroblasts using pre-miRs. *BAK1*, *BMF* and *BBC3* were downregulated 24-72 hours after transfection with downregulation of 0.41-0.74-fold ($p < 0.05$) in HC and SSc fibroblasts (Fig. 3C-D). These results indicate that miR-125b downregulation and overexpression directly affect the expression of its predicted targets.

Among these three genes of interest, BAK1 is the main regulator of apoptosis, while BMF and BBC3 play secondary roles in the mitochondrial apoptotic pathway. Based on the qPCR data, the miR-125b-dependent regulation of *BAK1* gene expression was the most consistent among all predicted targets. BAK1 protein expression was upregulated after miR-125b downregulation already 48 hours after transfection (median 2.19, $Q_{1,3}$ 1.52, 2.47, $p < 0.01$) and showed sustained upregulation up to 72 hours (median 2.28, $Q_{1,3}$ 1.66, 2.51, $p < 0.01$) (Fig. 4A) in HC fibroblasts. The maximal upregulation of BAK1 in SSc fibroblasts following miR-125b downregulation was noticed at 72 hours (median 2.61, $Q_{1,3}$ 1.96, 3.76, $p < 0.01$) (Fig. 4B). Overexpression of miR-125b decreased the expression of BAK1 in HC (median 0.38, $Q_{1,3}$ 0.23, 0.48, $p < 0.05$) and SSc fibroblasts (median 0.45, $Q_{1,3}$ 0.22, 0.61, $p < 0.05$) (Fig. 4C), indicating direct effects of miR-125b on BAK1 protein expression.

To further confirm BAK1 as the main target of miR-125b we analyzed the basal expression levels of BAK1 and two other targets (BMF and BBC3) in skin biopsies and dermal fibroblasts. We found that BAK1 is significantly upregulated in SSc skin (median 1.76, $Q_{1,3}$ 1.27, 2.14; $n = 9$, $p < 0.001$) compared with HC skin ($n = 13$) (Fig. 4D), as well as in SSc primary dermal fibroblasts (median 1.75, $Q_{1,3}$ 1.14, 3.13; $n = 13$, $p < 0.05$) compared with HC fibroblasts ($n = 10$) (Fig. 4E). There was no significant difference in the basal expression levels of BMF and BBC3 neither in skin nor in dermal fibroblasts (data not shown).

To implicate BAK1 as the main target of miR-125b and as a crucial mediator in apoptosis, we downregulated its expression with siRNA in HC and SSc dermal fibroblasts (Suppl. Fig. 7). We observed a significant reduction of apoptosis assessed by cleaved caspase 3 Western blot (Fig. 4F, G) and cleaved caspases 3/7 assay (Fig. 5F, G). These results clearly confirm that BAK1 represents a proapoptotic protein in primary dermal HC and SSc fibroblasts.

MiR-125b downregulation increases apoptosis and decreases proliferation

We hypothesized that the upregulation of apoptotic genes on the mRNA and protein level might influence the apoptosis rate of transfected cells. Accordingly, we performed the cleaved caspase 3/7 assay, which detects the cleaved effector caspases 3 and 7, assessing the final irreversible step of apoptosis. Since spontaneous apoptosis is a rare event in our experimental cell culture set-up, we used camptothecin and staurosporine to induce apoptosis. Downregulation of miR-125b increased the rate of apoptosis in cells already 24 hours after transfection (median 1.52, $Q_{1,3}$ 1.33, 1.82, $p < 0.01$, Fig. 5A). The higher rate of apoptosis persisted up to 72 hours after transfection in HC and SSc fibroblasts. To confirm the effects of miR-125b on apoptosis, we overexpressed miR-125b and observed reduced apoptosis starting from 24 hours after transfection (median 0.42, $Q_{1,3}$ 0.24, 0.62, $p < 0.01$) up to at least 72 hours (median 0.45, $Q_{1,3}$ 0.33, 0.7, $p < 0.01$) in HC and SSc fibroblasts (Fig. 5B).

To further verify the increased apoptosis in cells transfected with anti-125b, we performed Western blot and immunofluorescence staining for cleaved caspase 3. MiR-125b downregulation resulted in higher levels of cleaved caspase 3 in comparison with anti-scr controls in HC fibroblasts (median 2.29, $Q_{1,3}$ 1.62, 4.02) and in SSc fibroblasts (median 2.21, $Q_{1,3}$ 1.19, 4.09, $p < 0.01$) (Fig. 5C-D and Suppl. Fig. 8). Accordingly, overexpression of miR-125b caused a lower cleaved caspase 3 signal detected by Western blot (Fig. 5E), confirming that miR-125b downregulation activates cells to become more prone to undergo apoptosis and its overexpression dampens this process.

In order to elucidate the main target, through which miR-125b regulates apoptosis, we performed double transfection (downregulation of miR-125b expression with anti-125b and downregulation of BAK1 expression with siRNA) and further assessed apoptosis by cleaved caspases 3/7 assay. As expected, BAK1 downregulation alone decreased level of apoptosis in both HC and SSc fibroblasts after 48 hours post transfection. Indeed, double downregulation of miR-125b and BAK1 compared to anti-125b alone showed significantly lower rate of

apoptosis in HC and SSc fibroblasts after 48 (Fig. 5F-G) and 72 hours (Suppl. Fig. 9), indicating the crucial role of BAK1 in miR-125b-regulated apoptosis.

To further investigate the role of miR-125b in apoptosis, we performed Annexin V live staining after anti-125b transfection with and without apoptosis stimulation. Already 5 hours after staurosporine (STP)-induced apoptosis, increased signals of annexin V in cells transfected with anti-125b in comparison to anti-scr control were observed (Fig. 6A). This effect steadily increased for up to 16 hours with significant difference between 7 and 15 hours ($p < 0.05$) (Fig. 6B).

Additionally, we investigated the effects of mir-125b on proliferation of SSc fibroblasts by real-time proliferation assay. The cell index was monitored over 160 hours (Fig. 6C) and the slope of the exponential growth phase was used to assess proliferation. Following TGF β 1 stimulation, cells transfected with anti-125b showed decreased levels of proliferation compared to anti-scr controls ($n=8$, $p < 0.05$) (Fig. 6D). Similarly, reduced proliferation was also detected by BrdU assay in HC and in SSc fibroblasts after anti-125b transfection (median 0.83, $Q_{1,3}$ 0.71, 0.9, $p < 0.05$) (Suppl. Fig. 10).

Taken together, miR-125b downregulation, as observed in SSc skin biopsies and dermal SSc fibroblasts, increased apoptosis and reduced proliferation in dermal fibroblasts, indicating a regulatory role of miR-125b in fibrosis.

DISCUSSION

Our study showed that miR-125b is downregulated in the skin and primary dermal fibroblasts of SSc patients in comparison to healthy controls. Previously identified, downregulated miRs in SSc (let-7a, miR-7, miR-29, miR-133, etc.) directly de-repressed their ECM targets, such as collagens, thereby facilitating fibrogenesis(15, 16, 26-28). In contrast, we could demonstrate that miR-125b did not directly alter ECM components, namely collagens type I, III and V. Conversely, miR-125b downregulation resulted in a significantly decreased expression of α SMA, a marker of activated fibroblasts. Following miR-125b downregulation, less α SMA-positive fibers were observed, indicating that there is a reduced number of α SMA-positive cells, i.e. activated myofibroblasts. Such discrepancy might occur due to different molecular mechanisms of collagen production and formation of α SMA-positive fibers, even though both features usually appear together in emerging fibrosis. Neither collagen 1 nor α SMA are direct predicted targets of miR-125b, therefore, we assume

that reduced formation of α SMA-positive fibers may be a result of cytoskeleton reorganization due to entering pro-apoptotic status by the cells(29, 30) that will be discussed later. Thus, while previously identified, differentially expressed miRs in SSc promoted fibrosis, here we present a novel role for microRNAs in the pathophysiology of SSc: the downregulation of miR-125b in SSc exerts protective counter-regulatory effects on the progression of skin fibrosis

A recent publication showed that miR-125b was upregulated in cardiac fibrosis and in human primary cardiac fibroblasts (HCF)(17). This process was directly regulated by TGF β 1 and potentiated TGF β -induced collagen I and α SMA expression. At the same time, downregulation of miR-125b in HCF decreased TGF β -driven collagen I and α SMA expression(17). Consistent with these published data, in our studies on dermal fibroblasts, downregulation of miR-125b decreased TGF β -driven α SMA expression on the mRNA and protein level, but did not affect collagen I expression. Therefore, while downregulation of miR-125b in SSc skin may carry a compensatory, protective role against fibrosis, miR-125b upregulation in cardiac fibrosis appears to be pro-fibrotic. Such organ- and disease-specific functions are well-known features of miRs in general and specifically for miR-125b, for which pro- and anti-apoptotic effects in oncology have been proposed dependent on the underlying type of cancer(18).

We found that miR-125b expression in primary dermal fibroblasts is independent from major cytokines active in SSc. However, it is downregulated by inhibitors of histone deacetylases (HDAC), as shown by experiments with TSA (pan-inhibitor of HDAC) and TBA (inhibitor of class II HDAC with the greatest selectivity towards HDAC6(31)). Recent studies in oncology showed an upregulation of mir-125b by histone deacetylase inhibitors again pointing to tissue and disease-specific effects(32-35). Our results indicate the presence of an epigenetic repressor of miR-125b, which is activated by HDAC inhibitors. The detailed mechanisms underlying these effects need to be elucidated in further studies.

The limitation of our study is the lack of sufficient number of site matched healthy controls and of the subsets of the disease: lcSSc and dcSSc. Therefore, we used additionally unmatched healthy controls for analysis. Despite there may be a distinct gene expression pattern on the different sites of the body due to tissue origin and physiological conditions, as well as different gene expression signatures in disease subsets, there was no significant difference in miR-125b expression between different anatomical sites or between analyses of full skin or fibroblasts derived from lcSSc and dcSSc. These data allowed us to use also controls who were not matched for site of biopsy and pull together all patients' data.

To identify direct targets of miR-125b, we performed RNA deep sequencing that revealed *BAK1*, *BMF* and *BBC3* as potential predicted targets. Of note, all three consistently upregulated genes belong to the mitochondrial apoptotic pathway. Validation by qPCR showed that the downregulation of miR-125b increased the expression of these genes, whereas miR-125b overexpression resulted in their downregulation. These observations further support a direct functional regulation by miR-125b. Among the three genes of interest, *BAK1* had the strongest induction after miR-125b downregulation. Additionally, miR-125b overexpression led to downregulation of BAK1 protein both in HC and SSc fibroblasts. These results are further supported by other studies indicating a direct regulation of BAK1 by miR-125b(36-40).

One of the proposed mechanisms driving fibrosis in SSc and other related diseases is a lack of adequate fibroblast apoptosis(4). However, there is an incomplete understanding of the detailed mechanism underlying the activation of apoptosis during dermal fibrogenesis. Potential therapeutic strategies might be based on promoting apoptosis of pathological dermal myofibroblasts(41). We showed that miR-125b downregulation increases apoptosis, and that miR-125b upregulation decreases apoptosis, indicating the functional significance of miR-125b in the regulation of apoptosis in dermal fibroblasts. Furthermore, we showed by real-time proliferation assay and BrdU assay that miR-125b downregulation reduced cell proliferation in dermal fibroblasts, which is supported by studies in cancer (18, 42). However, if considered as an anti-fibrotic therapy, tissue and cell-specific differences of miR-125 will have to be addressed.

In conclusion, to our knowledge this is the first evidence that downregulation of a single miR in SSc has protective effects on disease progression. Downregulation of miR-125b may have compensatory protective effects directed against excessive skin fibrosis by (1) decreasing the number of α SMA-positive cells; (2) increasing apoptosis; and (3) decreasing proliferation in dermal fibroblasts.

REFERENCES

1. Khanna D, Distler JHW, Sandner P, Distler O. Emerging strategies for treatment of systemic sclerosis. *J Scleroderma Relat*. 2016;1(2):186-93.
2. Denton CP, Khanna D. Systemic sclerosis. *Lancet*. 2017;390(10103):1685-99.
3. Garret SM, Frost DB, Feghali-Bostwick C. The mighty fibroblast and its utility in scleroderma research. *J Scleroderma Relat Disord*. 2017;2(2):69-134.
4. Kissin E, Korn JH. Apoptosis and myofibroblasts in the pathogenesis of systemic sclerosis. *Curr Rheumatol Rep*. 2002;4(2):129-35.
5. Jelaska A, Korn JH. Role of apoptosis and transforming growth factor beta1 in fibroblast selection and activation in systemic sclerosis. *Arthritis Rheum*. 2000;43(10):2230-9.
6. Hotchkiss RS, Strasser A, McDunn JE, Swanson PE. Cell death. *N Engl J Med*. 2009;361(16):1570-83.
7. Santiago B, Galindo M, Rivero M, Pablos JL. Decreased susceptibility to Fas-induced apoptosis of systemic sclerosis dermal fibroblasts. *Arthritis Rheum*. 2001;44(7):1667-76.
8. Pena-Blanco A, Garcia-Saez AJ. Bax, Bak and beyond - mitochondrial performance in apoptosis. *FEBS J*. 2018;285(3):416-31.
9. Czabotar PE, Lessene G, Strasser A, Adams JM. Control of apoptosis by the BCL-2 protein family: implications for physiology and therapy. *Nat Rev Mol Cell Biol*. 2014;15(1):49-63.
10. Horsburgh S, Fullard N, Roger M, Degnan A, Todryk S, Przyborski S, et al. MicroRNAs in the skin: role in development, homeostasis and regeneration. *Clin Sci (Lond)*. 2017;131(15):1923-40.
11. Kim VN, Han J, Siomi MC. Biogenesis of small RNAs in animals. *Nat Rev Mol Cell Biol*. 2009;10(2):126-39.
12. Vettori S, Gay S, Distler O. Role of MicroRNAs in Fibrosis. *Open Rheumatol J*. 2012;6:130-9.
13. Bartel DP. MicroRNAs: genomics, biogenesis, mechanism, and function. *Cell*. 2004;116(2):281-97.
14. Li H, Yang R, Fan X, Gu T, Zhao Z, Chang D, et al. MicroRNA array analysis of microRNAs related to systemic scleroderma. *Rheumatol Int*. 2012;32(2):307-13.
15. Honda N, Jinnin M, Kajihara I, Makino T, Makino K, Masuguchi S, et al. TGF-beta-mediated downregulation of microRNA-196a contributes to the constitutive upregulated type I collagen expression in scleroderma dermal fibroblasts. *J Immunol*. 2012;188(7):3323-31.
16. Makino K, Jinnin M, Hirano A, Yamane K, Eto M, Kusano T, et al. The downregulation of microRNA let-7a contributes to the excessive expression of type I collagen in systemic and localized scleroderma. *J Immunol*. 2013;190(8):3905-15.
17. Nagpal V, Rai R, Place AT, Murphy SB, Verma SK, Ghosh AK, et al. MiR-125b Is Critical for Fibroblast-to-Myofibroblast Transition and Cardiac Fibrosis. *Circulation*. 2016;133(3):291-301.
18. Banzhaf-Strathmann J, Edbauer D. Good guy or bad guy: the opposing roles of microRNA 125b in cancer. *Cell Commun Signal*. 2014;12:30.
19. Le MT, Shyh-Chang N, Khaw SL, Chin L, Teh C, Tay J, et al. Conserved regulation of p53 network dosage by microRNA-125b occurs through evolving miRNA-target gene pairs. *PLoS Genet*. 2011;7(9):e1002242.
20. Zhang L, Ge Y, Fuchs E. miR-125b can enhance skin tumor initiation and promote malignant progression by repressing differentiation and prolonging cell survival. *Genes Dev*. 2014;28(22):2532-46.

21. van den Hoogen F, Khanna D, Fransen J, Johnson SR, Baron M, Tyndall A, et al. 2013 classification criteria for systemic sclerosis: an American college of rheumatology/European league against rheumatism collaborative initiative. *Ann Rheum Dis*. 2013;72(11):1747-55.
22. LeRoy EC, Black C, Fleischmajer R, Jablonska S, Krieg T, Medsger TA, Jr., et al. Scleroderma (systemic sclerosis): classification, subsets and pathogenesis. *J Rheumatol*. 1988;15(2):202-5.
23. Iwamoto N, Vettori S, Maurer B, Brock M, Pachera E, Jungel A, et al. Downregulation of miR-193b in systemic sclerosis regulates the proliferative vasculopathy by urokinase-type plasminogen activator expression. *Ann Rheum Dis*. 2016;75(1):303-10.
24. Chen C, Ridzon DA, Broomer AJ, Zhou Z, Lee DH, Nguyen JT, et al. Real-time quantification of microRNAs by stem-loop RT-PCR. *Nucleic Acids Res*. 2005;33(20):e179.
25. Distler JH, Jungel A, Huber LC, Schulze-Horsel U, Zwerina J, Gay RE, et al. Imatinib mesylate reduces production of extracellular matrix and prevents development of experimental dermal fibrosis. *Arthritis Rheum*. 2007;56(1):311-22.
26. Maurer B, Stanczyk J, Jungel A, Akhmetshina A, Trenkmann M, Brock M, et al. MicroRNA-29, a key regulator of collagen expression in systemic sclerosis. *Arthritis Rheum*. 2010;62(6):1733-43.
27. Etoh M, Jinnin M, Makino K, Yamane K, Nakayama W, Aoi J, et al. microRNA-7 down-regulation mediates excessive collagen expression in localized scleroderma. *Arch Dermatol Res*. 2013;305(1):9-15.
28. Honda N, Jinnin M, Kira-Etoh T, Makino K, Kajihara I, Makino T, et al. miR-150 down-regulation contributes to the constitutive type I collagen overexpression in scleroderma dermal fibroblasts via the induction of integrin beta3. *Am J Pathol*. 2013;182(1):206-16.
29. Povea-Cabello S, Oropesa-Avila M, de la Cruz-Ojeda P, Villanueva-Paz M, de la Mata M, Suarez-Rivero JM, et al. Dynamic Reorganization of the Cytoskeleton during Apoptosis: The Two Coffins Hypothesis. *Int J Mol Sci*. 2017;18(11).
30. Shinde AV, Humeres C, Frangogiannis NG. The role of alpha-smooth muscle actin in fibroblast-mediated matrix contraction and remodeling. *Biochim Biophys Acta Mol Basis Dis*. 2017;1863(1):298-309.
31. Butler KV, Kalin J, Brochier C, Vistoli G, Langley B, Kozikowski AP. Rational design and simple chemistry yield a superior, neuroprotective HDAC6 inhibitor, tubastatin A. *J Am Chem Soc*. 2010;132(31):10842-6.
32. Chen YJ, Wang WH, Wu WY, Hsu CC, Wei LR, Wang SF, et al. Novel histone deacetylase inhibitor AR-42 exhibits antitumor activity in pancreatic cancer cells by affecting multiple biochemical pathways. *PLoS One*. 2017;12(8):e0183368.
33. Cisneros-Soberanis F, Andonegui MA, Herrera LA. miR-125b-1 is repressed by histone modifications in breast cancer cell lines. *Springerplus*. 2016;5(1):959.
34. Shen T, Sanchez HN, Zan H, Casali P. Genome-Wide Analysis Reveals Selective Modulation of microRNAs and mRNAs by Histone Deacetylase Inhibitor in B Cells Induced to Undergo Class-Switch DNA Recombination and Plasma Cell Differentiation. *Front Immunol*. 2015;6:627.
35. Wang S, Huang J, Lyu H, Lee CK, Tan J, Wang J, et al. Functional cooperation of miR-125a, miR-125b, and miR-205 in entinostat-induced downregulation of erbB2/erbB3 and apoptosis in breast cancer cells. *Cell Death Dis*. 2013;4:e556.
36. Micheli F, Palermo R, Talora C, Ferretti E, Vacca A, Napolitano M. Regulation of proapoptotic proteins Bak1 and p53 by miR-125b in an experimental model of Alzheimer's disease: Protective role of 17beta-estradiol. *Neurosci Lett*. 2016;629:234-40.

37. Kong F, Sun C, Wang Z, Han L, Weng D, Lu Y, et al. miR-125b confers resistance of ovarian cancer cells to cisplatin by targeting pro-apoptotic Bcl-2 antagonist killer 1. *J Huazhong Univ Sci Technolog Med Sci.* 2011;31(4):543-9.
38. Chen X, Liu J, Feng WK, Wu X, Chen SY. MiR-125b protects against ethanol-induced apoptosis in neural crest cells and mouse embryos by targeting Bak 1 and PUMA. *Exp Neurol.* 2015;271:104-11.
39. Chen J, Fu X, Wan Y, Wang Z, Jiang D, Shi L. miR-125b inhibitor enhance the chemosensitivity of glioblastoma stem cells to temozolomide by targeting Bak1. *Tumour Biol.* 2014;35(7):6293-302.
40. Li Q, Wu Y, Zhang Y, Sun H, Lu Z, Du K, et al. miR-125b regulates cell progression in chronic myeloid leukemia via targeting BAK1. *Am J Transl Res.* 2016;8(2):447-59.
41. Lagares D, Santos A, Grasberger PE, Liu F, Probst CK, Rahimi RA, et al. Targeted apoptosis of myofibroblasts with the BH3 mimetic ABT-263 reverses established fibrosis. *Sci Transl Med.* 2017;9(420).
42. Fan YX, Bian XH, Qian PD, Chen ZZ, Wen J, Luo YH, et al. MicroRNA-125b inhibits cell proliferation and induces cell apoptosis in esophageal squamous cell carcinoma by targeting BMF. *Oncol Rep.* 2018.

FIGURE LEGENDS

Figure 1. Downregulation of miR-125b in skin samples and primary dermal fibroblasts.

A. MiR-125b expression in skin biopsies from healthy controls (HC) and SSc patients (n=10 each, black triangles indicate dcSSc subset). **B.** Basal expression of miR-125b in cultured primary dermal fibroblasts from HC and SSc (n=10 each). **C-H.** Histone deacetylase inhibitors (HDAC) regulate miR-125b expression. **C.** HC fibroblasts (n = 5) and **D.** SSc fibroblasts (n=5) were stimulated with different doses of HDAC inhibitor trichostatin A (TSA) for 24 hours. **E.** HC (n = 6) and **F.** SSc fibroblasts (n=5) were stimulated with 2μM TSA for up to 72 hours. **G.** HC fibroblasts (n = 7) and **H.** SSc fibroblasts (n=7) were stimulated with different doses of HDAC inhibitor tubastatin A (TBA) for 24 hours. **I-J.** Effect of TBA on the expression of unrelated miR-342. **I.** HC (n = 7) and **J.** SSc fibroblasts (n=7) were stimulated with different doses of TBA for 24 hours. Red lines represent respective controls and red dashed lines represent the median level of miR-125b downregulation in SSc fibroblasts. **A-J.** Data are presented as median ± interquartile range. ***p<0.001, **p<0.01, *p<0.05, ns – not significant, **A-B.** ***p < 0.001, Mann-Whitney test. **C.-J.** ANOVA, Dunnett's test.

Figure 2. α SMA expression is regulated by miR-125b after TGF β stimulation. A-B. *ACTA2* mRNA expression after transfection with anti-125b and TGF β (10ng/ml) stimulation in HC fibroblasts **A.** without (n=6) and **B.** with starvation (n=5). RNA was harvested 4 days after transfection, 3 days of starvation (only **B**) and 2 days of TGF β stimulation. **C-D.** Representative pictures of Western blot and semi-quantification with densitometry analyzed by ImageJ for α SMA from HC fibroblasts **C.** without starvation (n=6) and **D.** with starvation (n=6) 5 days after transfection, 4 days of starvation (only **D**) and 3 days of TGF β stimulation (**C-D**). Data are presented as median \pm interquartile range. ns – not significant, *p<0.05, Mann-Whitney test. **E.** α SMA immunofluorescence after transfection with anti-125b and TGF β stimulation in HC fibroblasts (n=4). Red – α SMA, blue – DAPI. Scale bar 100 μ m. **F – G.** Representative pictures of Western blot and semi-quantification with densitometry analyzed by ImageJ for α SMA from SSc fibroblasts transfected **F.** with anti-125b (n=8) and **G.** pre-125b (n=5) 5 days after transfection, 4 days of starvation and 3 days of TGF β stimulation. Data are presented as median \pm interquartile range. ns – not significant, **p<0.01, Mann-Whitney test.

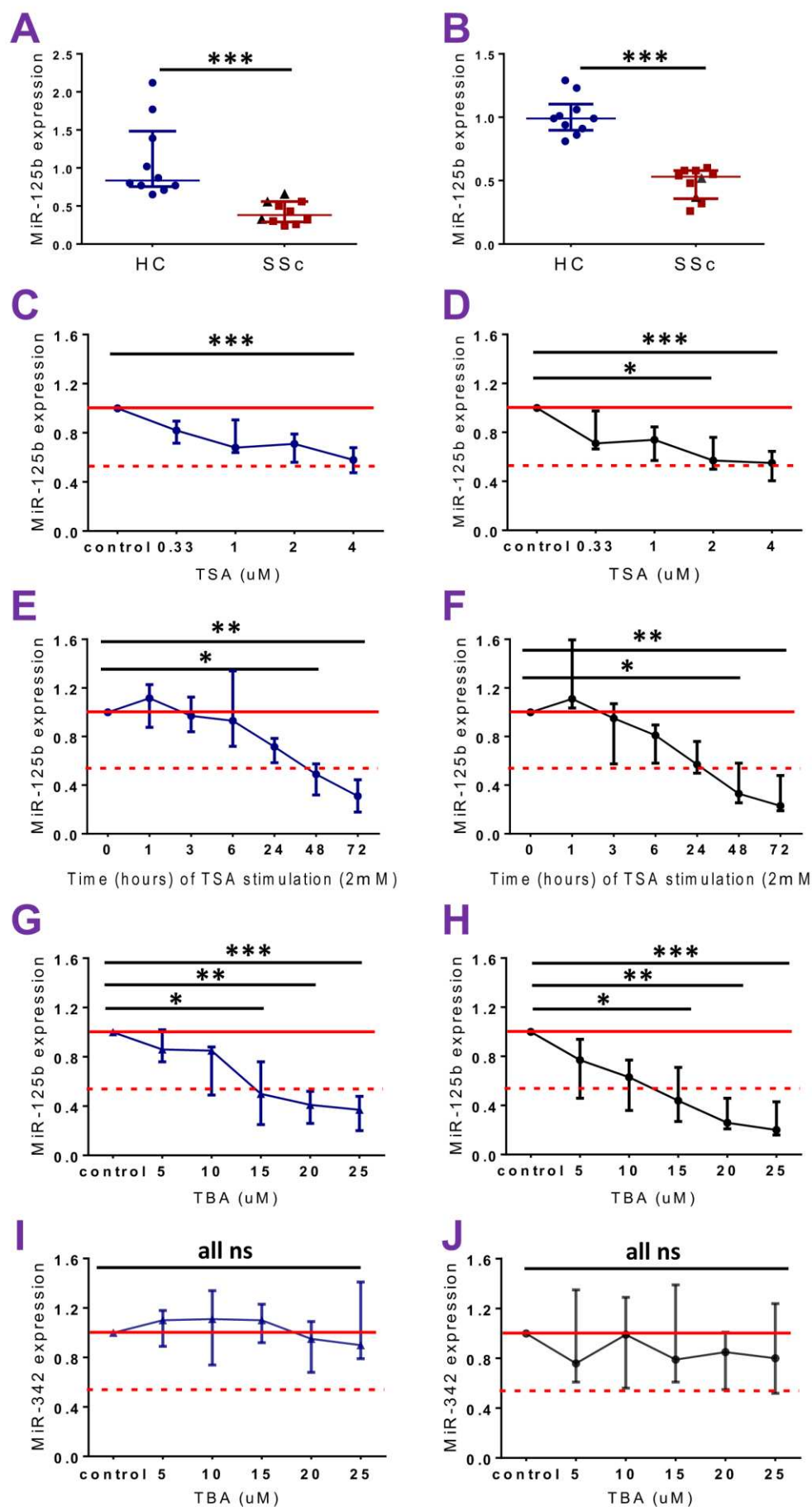
Figure 3. MiR-125b regulates the expression of its pro-apoptotic targets *BAK1*, *BMF* and *BBC3*. **A.** *BAK1*, *BMF* and *BBC3* mRNA expression 24, 48 and 72 hours after transfection with anti-125b in HC fibroblasts (n=12 for each time point). **B.** *BAK1*, *BMF* and *BBC3* mRNA expression 24, 48 and 72 hours after transfection with anti-125b in SSc fibroblasts (n=12 for each time point). **C.** *BAK1*, *BMF* and *BBC3* mRNA expression 24, 48 and 72 hours after pre-125b transfection in HC fibroblasts (n=12 for each time point). **D.** *BAK1*, *BMF* and *BBC3* mRNA expression 24, 48 and 72 hours after pre-125b transfection in SSc fibroblasts (n=12 for each time point). Data are presented as median \pm interquartile range. Red lines represent respective anti-scr controls. ***p<0.01, **p<0.01, *p<0.05, ns – not significant, Wilcoxon signed rank test.

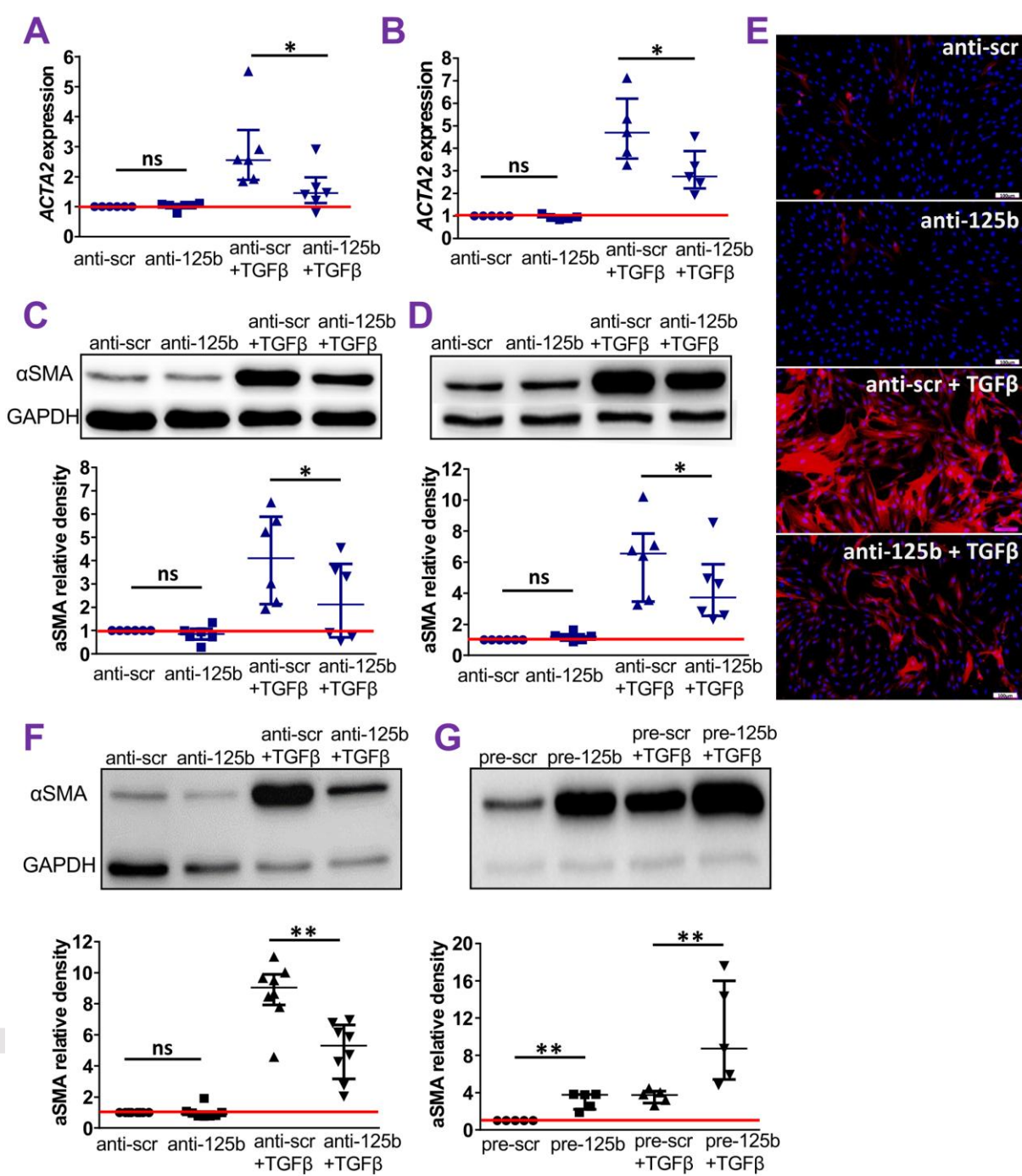
Figure 4. MiR-125b regulates pro-apoptotic BAK1 protein expression. Representative pictures of Western blot and semi-quantification with densitometry analyzed by ImageJ for BAK1 from **A.** HC (n=10) and **B.** SSc (n=10) fibroblasts (48 hours after transfection with anti-125b). **C.** Representative pictures of Western blots and semi-quantification from HC (n=6) and SSc (n=8) fibroblasts 48 hours after transfection with pre-125b. Data are presented as median \pm interquartile range. Red lines represent respective controls. **p<0.01, *p<0.05, Wilcoxon signed rank test. **D.** BAK1 expression in skin biopsies from HC (n=13) and SSc

patients (n=9). **E.** Basal expression of BAK1 in cultured primary dermal fibroblasts from HC (n=10) and SSc (n=13). * $p < 0.05$, *** $p < 0.001$, Mann-Whitney test. **F-G.** Western blot for cleaved caspase 3. Representative pictures of Western blot and semi-quantification by ImageJ for cleaved caspase 3 from **F.** HC (n=7) and **G.** SSc (n=7) fibroblasts transfected with BAK1 siRNA. Data are presented as median \pm interquartile range. Red lines represent respective controls. * $p < 0.05$, Wilcoxon signed rank test.

Figure 5. Cleaved caspases 3/7 is regulated by miR-125b and BAK1. A-B. Analysis of cleaved caspases 3/7 measured by Real-Glo® assay. **A.** Camptothecin (CPT) induced apoptosis 24, 48 and 72 hours after anti-125b transfection in HC (n=10) and in SSc fibroblasts (n=9). **B.** CPT-induced apoptosis 24, 48 and 72 hours after transfection with pre-125b in HC (n=10) and in SSc fibroblasts (n=9). 200 μ M CPT was added 18 hours before the assay to induce apoptosis. **C-E.** Western blot for cleaved caspase 3. **C-D.** Representative pictures of Western blot and semi-quantification by ImageJ for cleaved caspase 3 from **C.** HC (n=10) and **D.** SSc (n=10) fibroblasts transfected with anti-125b. **E.** Representative pictures of Western blot and semi-quantification from HC (n=3) and SSc (n=3) fibroblasts transfected with pre-125b; significance is not tested due to low n . **F-G.** Cleaved caspases 3/7 assay in **F.** HC (n=8) and in **G.** SSc fibroblasts (n=7). CPT induced apoptosis was assessed 48 hours after double anti-125b and BAK1 siRNA transfection. **A-G.** Data are presented as median \pm interquartile range and normalized to respective scrambled control. Red lines represent respective controls. *** $p < 0.01$, ** $p < 0.01$, * $p < 0.05$, Wilcoxon signed rank test.

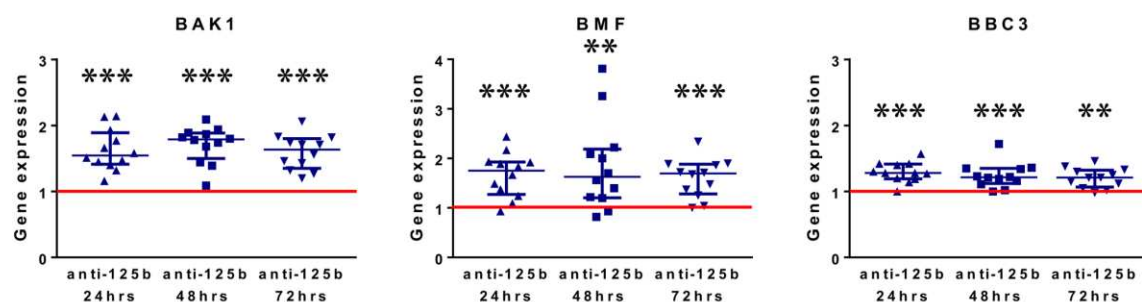
Figure 6. MiR-125b activates apoptosis with the reduction of cell proliferation. A. Representative picture of annexin V live measurements normalized to anti-scr. **B.** Statistical analysis of annexin V live measurements (n=6 SSc) for each time point recorded (every 70 min) after anti-125b transfection normalized to respective anti-scr controls (represented by the red line). Data are presented as median \pm interquartile range. * $p < 0.05$, ns – not significant, Wilcoxon signed rank test. **C.** Representative picture of real-time proliferation assessed by cell index normalized to the time point of transfection. **D.** Slope was used to assess the proliferation (n=8, SSc fibroblasts). Data are presented as median \pm interquartile range. * $p < 0.05$, ns – not significant, Wilcoxon matched-pairs signed rank test.





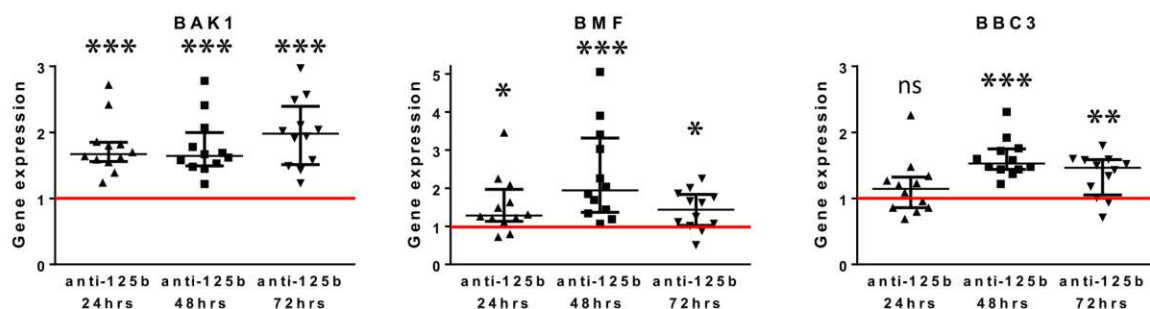
A

Effect of anti-125b transfection on HC fibroblasts



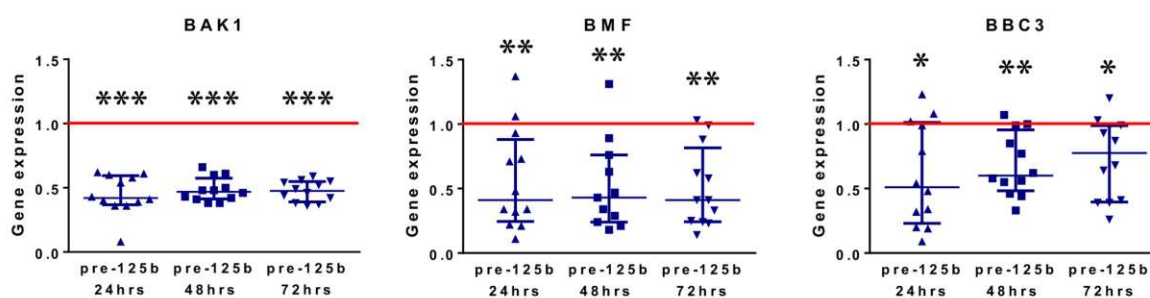
B

Effect of anti-125b transfection on SSc fibroblasts



C

Effect of pre-125b transfection on HC fibroblasts



D

Effect of pre-125b transfection on SSc fibroblasts

